BMC Medical Imaging

RESEARCH Open Access

Combining artificial intelligence assisted image segmentation and ultrasound based radiomics for the prediction of carotid plaque stability

Jiajia Song[1†], Liwen Zou[2†], Yu Li[3], Xiaoyin Wang[4], Junlan Qiu[5*] and Kailin Gong[1*]

Abstract

Purpose Utilizing artificial intelligence (AI) technology for the segmentation of plaques on ultrasound images to evaluate the stability of carotid artery plaques and analyze its diagnostic accuracy in differentiating vulnerable plaques from stable ones.

Methods A retrospective study was conducted on 202 patients with ischemic stroke, who were divided into vulnerable plaque group (85 cases) and stable plaque group (117 cases) based on the results of carotid color Doppler ultrasound examination. From the vulnerable plaque group, 63 cases were randomly selected as the modeling group and 22 cases as the validation group; similarly, from the stable plaque group, 87 cases were randomly selected as the modeling group and 30 cases as the validation group. Based on the ultrasound images of the modeling group, plaques were segmented using artificial intelligence technology, and 1414 radiomics features were extracted. These features were then subjected to dimensionality reduction and feature selection using the least absolute shrinkage and selection operator (LASSO) method. Subsequently, a Support Vector Machine (SVM) model was constructed and validated using the selected features. The sensitivity, specificity, and Area Under the Curve (AUC) of the model were evaluated through the analysis of the receiver operating characteristic (ROC) curve.

Results A total of 43 radiomics feature parameters were selected by the LASSO method. The training group for the SVM model had an AUC of 89.42% (95% CI: 80.74-98.10%), sensitivity of 79.84%, and specificity of 93.10%, while the validation group had an AUC of 82.73% (95% CI: 71.64-93.81%), sensitivity of 81.82%, and specificity of 80.00%.

[†]Jiajia Song and Liwen Zou are co-first authors.

Kailin Gong is the main corresponding author.

*Correspondence:
Junlan Qiu
weiyumo@163.com
Kailin Gong
kelly3328218@163.com

Full list of author information is available at the end of the article

Conclusion The use of artificial intelligence technology for the segmentation of plaques in ultrasound images, coupled with the analysis of radiomics models, can efficiently distinguish the stability of carotid artery plaques, providing a diagnostic basis for the clinical prediction of ischemic stroke.

Clinical trial number Not applicable.

Keywords Ischemic stroke, Carotid plaque, Image segmentation, Artificial intelligence, Radiomics, Stability assessment

Introduction

Stroke is one of the leading causes of disability and mortality worldwide, with its high incidence, prevalence, disability, and fatality rates remaining a focal point of medical research [1, 2]. Among them, ischemic stroke is particularly common. The pathogenesis of ischemic stroke is complex, involving various pathophysiological factors such as atherosclerosis, thrombosis, small artery occlusion, and other vascular diseases, as well as cardiac diseases and systemic metabolic diseases like hypertension and diabetes [3–5]. Atherosclerosis is an important common cause, characterized by plaque formation that leads to vascular stenosis, and triggers inadequate blood perfusion in brain tissue, with the carotid artery being the most commonly affected [6]. As early as 1989, Muller introduced the concept of the "vulnerable plaque," which, due to its instability and propensity for rupture, has become a focus of attention in the medical community [7]. Vulnerable plaques have a series of significant structural features, such as active inflammatory responses, large lipid cores, thin fibrous caps, and ruptures, internal bleeding, or ulcers on the plaque surface [8–10]. Once the plaque ruptures, thrombi enter the intracranial arteries with blood flow, triggering occlusive events and causing severe brain damage. Therefore, early identification and assessment of the stability of carotid plaques are of great significance for the prevention of ischemic stroke [11].

With the advancement of medical imaging technology, various imaging methods such as Ultrasonography (US), multi-slice spiral CT angiography (MSCTA), and magnetic resonance imaging (MRI) have been employed for the assessment of carotid plaques, providing information on morphology, histology, and hemodynamics of the plaques [12, 13]. Carotid ultrasound has become the preferred method of examination due to its simplicity, low cost, and high diagnostic accuracy rate. However, traditional ultrasound examination has limitations in the diagnosis of vulnerable plaques, such as restrictions in the operation angle, differences in physician experience, and the complexity of plaque morphology and composition, leading to low diagnostic efficiency. Therefore, there is an urgent need for new technologies to assist sonographers in improving the accuracy and efficiency of diagnosis [14].

Artificial intelligence (AI) technology has brought breakthroughs in the field of medical image analysis. AI technology, combined with algorithms such as Convolutional Neural Networks (CNNs) and Variational Autoencoders (VAEs), has significantly advanced image analysis techniques. Recent surveys have highlighted the significant progress in AI-based segmentation and analysis of medical images, particularly in the context of deep learning techniques [15, 16]. AI-based ultrasound image plaque segmentation technology utilizes deep learning algorithms to automatically segment and assess carotid plaques, enhancing the accuracy and efficiency of the assessment [17, 18]. Recent advances in deep learning-based segmentation for ultrasound images have shown significant potential in improving diagnostic accuracy and efficiency [19]. Additionally, clinical perspectives on ultrasound imaging of carotid plaque vulnerability highlight the importance of these techniques in clinical settings [20].

Radiomics, which integrates digital image processing techniques, statistics, and machine learning, conducts quantitative and high-throughput analyses of medical images, aiding in the differentiation between carotid vulnerable plaques and stable plaques [21]. A systematic review of radiomics in predicting carotid plaque vulnerability has shown that multi-modal imaging approaches can significantly enhance the accuracy of vulnerability assessment [22, 23].

This study aims to explore the application of AI-based ultrasound image plaque segmentation technology in the stability assessment of carotid plaques, as well as the potential of radiomics in distinguishing between vulnerable and stable carotid plaques, providing more effective tools for the early identification, risk assessment, and treatment decision-making of ischemic stroke. With the continuous development of medical imaging technology and AI, we hope to provide more precise diagnostic tools and treatment strategies to better prevent and manage ischemic stroke.

Materials and methods

Design of the study

This study was designed as a retrospective diagnostic accuracy study, aiming to evaluate the performance of an AI-assisted image segmentation and ultrasound

(US)-based radiomics approach in predicting the stability of carotid artery plaques. The sample size was determined based on a comprehensive consideration of the study objectives, data availability, and experience from previous studies. A non-random sampling method stratified by time was employed. The primary output of the model established in this study was the probability of US images being classified as vulnerable, with the endpoint variable being the diagnostic label of vulnerable/non-vulnerable. The measurement indicators included sensitivity, specificity, positive predictive value (PPV), negative predictive value (NPV), and area under the curve (AUC). The study adhered to the Standards for Reporting Diagnostic Accuracy (STARD) guidelines to ensure transparency and reproducibility in reporting diagnostic test accuracy.

Study population

The research was performed in accordance with relevant guidelines and regulations, and granted ethical approval by the review board of Affiliated Nanjing Brain Hospital, Nanjing Medical University. For this retrospective study, obtaining informed consent was exempted. The retrospective analysis was conducted on patients with ischemic stroke treated at Affiliated Nanjing Brain Hospital, Nanjing Medical University from January 1, 2022, to December 31, 2023. MRI and ultrasound data were obtained from the hospital's data system. Inclusion criteria: (1) diagnosed with ischemic stroke through clinical and magnetic resonance imaging examinations; (2) the diagnosis of ischemic stroke met the criteria set forth in the "Chinese Guidelines for the Diagnosis and Treatment of Ischemic Stroke" published by the Chinese Medical Association in 2018 [24]; (3) all patients underwent carotid ultrasound examination. Exclusion criteria were shown as follows: (1) patients with unclear diagnosis of ischemic stroke; (2) patients who failed to complete magnetic resonance and carotid ultrasound examinations; (3) patients with severe heart disease, kidney disease, cancer, autoimmune diseases, mental disorders; (4) patients with other neurological diseases.

Figure 1 displays the flowchart of the study population. Patients diagnosed with ischemic stroke from January 1, 2022, to December 31, 2022, were included in the training cohort, and those diagnosed from January 1, 2023, to December 31, 2023, were included in the validation cohort. The training and validation cohorts comprised 150 patients and 52 patients, respectively.

US examination

In this study, carotid plaque detection was performed using the EPIQ5 and EPIQ7 series of color Doppler ultrasound diagnostic equipment produced by the Dutch company PHILIPS, with a transducer frequency of 7.5–12.0 MHz. During the ultrasound examination, subjects were placed in a supine position with their heads slightly elevated to improve image clarity. The working frequency of the ultrasound transducer was set between 7.5 and 12.0 MHz to ensure a detailed examination of the common carotid artery, internal carotid artery, and external carotid artery. The primary step of the examination was to accurately locate the common carotid artery, followed by a gradual upward scan to the intracranial entrance of the internal carotid artery. Based on the morphological characteristics of the plaques, this study classified plaques into four types [25]: Type I is characterized by eccentric thickening of the intima, with local protrusions less than 2 millimeters and flat plaques with rough, medium-strength echo; Type II is a soft plaque with a thickness greater than 2 millimeters and uneven echo; Type III is a hard plaque with strong echo and acoustic shadow; Type IV is an ulcerative plaque with an irregular surface and hypoechoic edges. In this study, Type II and IV plaques were defined as vulnerable plaques, while Type I and III plaques were defined as stable plaques. This classification method helps clinicians more accurately assess the stability of carotid plaques, providing key information for the prevention and treatment of ischemic stroke.

Image post-processing

Using an artificial intelligence-based image segmentation method, operations are performed on the software MATLAB. All subjects' raw data are imported into the computer, and double line detection (DLD) is applied to the local segmentation of this edge mapping. The calculated contours are used as input for the snake segmentation model. Currently, most radiomics methods manually extract the region of interest (ROI) from ultrasound images [26, 27]. This study proposes an automatic preprocessing segmentation method, transforming the superpixel-level optical flow and binary mask features into regular probability superpixels, used to construct a superpixel-level conditional random field, automatically labeling the lumen (foreground, i.e., ROI) and other tissues (background) [28–30]. An improved mathematical model is used for plaque segmentation within the ROI [30, 31]. Figure 2 presents two segmentation examples.

Radiomics

Two ultrasonographers, each with over a decade of experience in interpreting neck ultrasound images, independently analyzed the artificially segmented plaque ultrasound images. The obtained images were imported into self-developed software (Image Analyzer 2.0, China), from which 1414 radiomics features could be extracted from each region of interest (ROI), categorized into the following three types [32–35]: (1)First-order features:

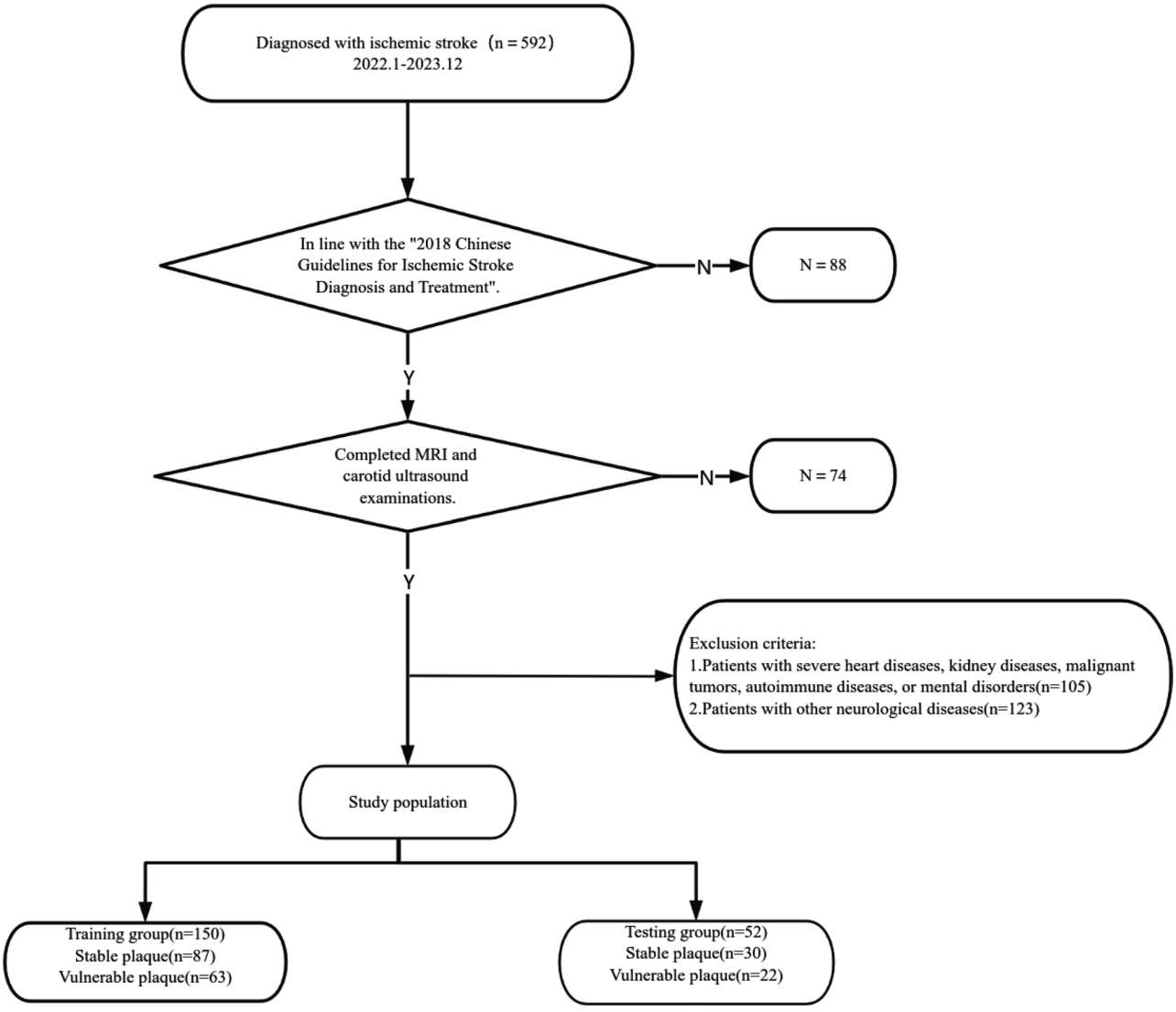

Fig. 1 Flow chart of enrolling the study population

Statistical features, i.e., gray-level histogram features, reflecting the frequency distribution of gray-level values within the ROI, with a total of 20 features extracted; where N represents the total number of gray-level values within the ROI, P(i) represents the frequency of a certain value within the ROI, and X(i) represents the count of occurrences within the ROI. Classification as follows:

1)

$$\text{Mean} = \frac{1}{N}\sum_{i}^{N} X(i)$$

2)

$$\text{Standard deviation} = \sqrt{\frac{1}{1-N}\sum_{i-1}^{N}\left(X(i)-\bar{X}\right)^{2}}$$

3)

$$\text{Skewness} = \frac{\frac{1}{N}\sum_{i}^{N} X(i)-\bar{X})^{3}}{\left[\sqrt{\frac{1}{1-N}\sum_{i-1}^{N}\left(X(i)-\bar{X}\right)^{2}}\right]^{3}}$$

4)

$$\text{Kurtosis} = \frac{\frac{1}{N}\sum_{i}^{N} X(i)-\bar{X})^{4}}{\left(\frac{1}{1-N}\sum_{i-1}^{N}\left(X(i)-\bar{X}\right)^{2}\right)^{2}}$$

5)

$$\text{Entropy} = \sum_{\text{i=1}}^{\text{N}_1} \text{p (i)log2 p(i)}$$

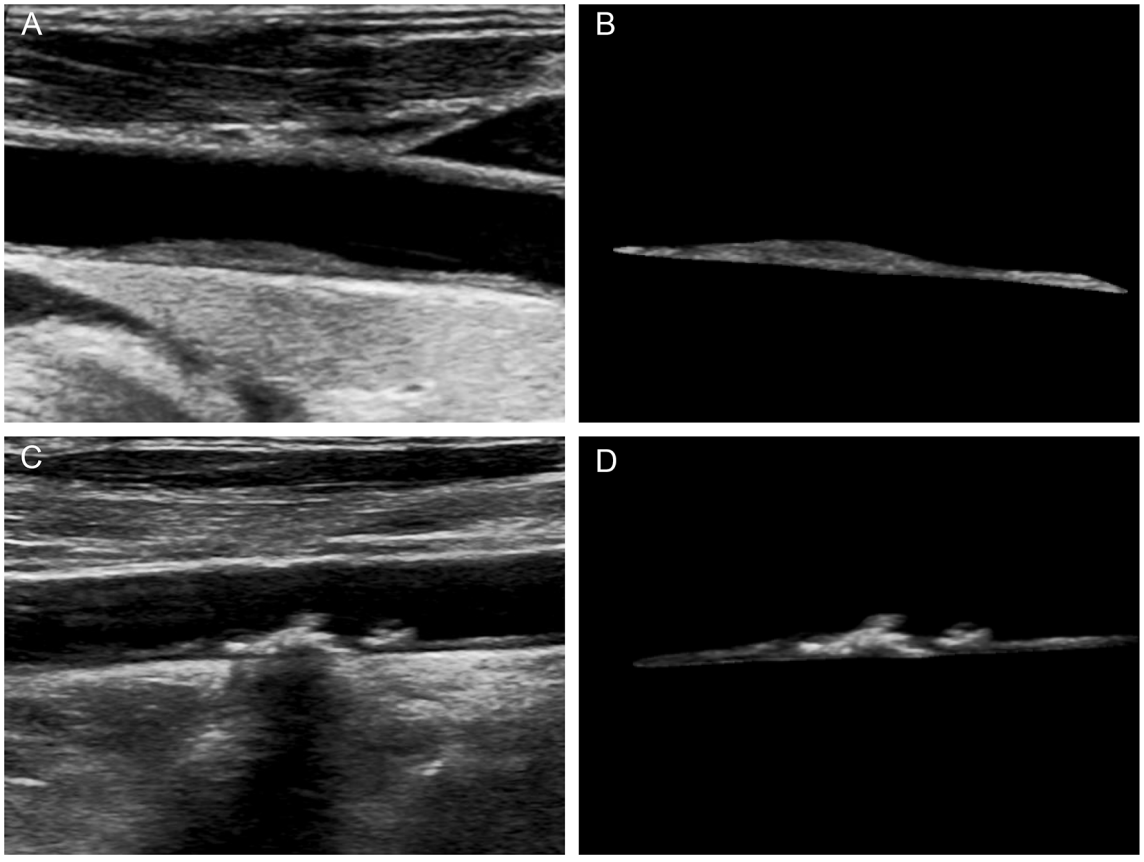

Fig. 2 Vulnerable and stable plaques in carotid ultrasound images before and after artificial intelligence segmentation. **A**: Stable plaques in ultrasound images; **B**: Artificial intelligence-segmented stable plaques; **C**: Vulnerable plaques in ultrasound images; **D**: Artificial intelligence-segmented vulnerable plaques

6) Max frequency: The maximum frequency that appears in X.
7) Mode: Peak gray level in histogram.
8) Min.
9) Max.
10) Percentile n%.
11) Histogram width.
12) AUC low: Proportion of gray levels below 25% percentile (excluding top and bottom 1%).
13) s-sDlowest: First gray level with count 5 along the positive x-axis.
14) s-sDav distribution witdh: Histogram width at half-peak value.

Shape features, which mainly describe the size and shape characteristics of the ROI, with a total of 11 features extracted, including volume, surface area, maximum diameter, surface-volume ratio, sphericity, spherical disproportion, compactness, etc. (2) Second-order features: Textural features, describing the spatial relationships between different voxels and the shapes of texture patterns. Texture features are derived from the gray-level co-occurrence matrix (GLCM) and the gray-level run length matrix (GLRLM). Texture features based on GLCM: This method involves calculating the GLCM, which depicts the frequency distribution of a pair of gray-level values along a specific direction ($\theta = 0°$, 45°, 90°, 135°, or random angles) at a certain distance; a total of 208 feature parameters are extracted.(3)Third-order features: Texture features based on GLRLM, calculating the matrix of continuous voxels of the same gray-level value along a pre-set direction ($\theta = 0°$, 90°, or random direction), with a total of 130 feature parameters extracted.

Statistical analysis

In this study, descriptive statistical analysis was performed for quantitative data, with mean and standard deviation calculated and presented as mean ± standard deviation ($x \pm s$). The t-test was used to compare differences between groups. For qualitative data, categories were encoded as numerical values, and frequency distribution tables were used to count the occurrences of each category. The chi-square test was employed to compare differences between groups. During the statistical analysis, we first conducted tests for normality and homogeneity of variance to ensure that the selected statistical

methods met their underlying assumptions. If the data did not meet the assumptions of normality or homogeneity of variance, we applied appropriate non-parametric tests (such as the Mann-Whitney U test or Kruskal-Wallis test) or performed data transformations (e.g., logarithmic transformation). Data analysis was conducted using SPSS version 25.0, and a p-value less than 0.05 was considered statistically significant.

The least absolute shrinkage and selection operator (LASSO) model is used to select radiomics features from artificially segmented plaque ultrasound images.

Table 1 Clinical and demographic characteristics of the training and validation cohorts

		Training cohorts *n*=150	Validation cohorts *n*=52	*p*
Gender				0.258
	Male	70	29	
	Female	80	23	
BMI				0.002
	< 18.5	1	1	
	18.5–24.9	41	13	
	25.0-29.9	78	22	
	> 30.0	30	16	
Hypertension				0.262
	yes	10	6	
	no	140	46	
Diabetes				0.001
	yes	92	20	
	no	58	32	
Hyperlipidemia				0.003
	yes	9	10	
	no	141	42	
Coronary heart disease				0.472
	yes	33	9	
	no	117	43	
IMT				0.014
	< 1.0	35	4	
	≥ 1.0	115	48	
Lumen				0.021
	normal	124	35	
	mild stenosis	19	10	
	moderate stenosis	5	5	
	severe stenosis	2	2	
	occlusion	0	0	
PSV				0.031
	normal	128	34	
	accelerated	17	15	
	decelerated	5	3	
PSV ratio				0.099
	<2	143	45	
	2–4	5	5	
	>4	2	2	

The radiomics features selected by LASSO regression are further modeled and validated using a kernel function support vector machine (SVM). The predictive performance of the model is evaluated using the receiver operating characteristic curve (ROC) analysis, recording the area under the curve (AUC), optimal threshold, sensitivity, specificity, positive predictive value, and negative predictive value. Image preprocessing and radiomic feature extraction were implemented by the open-source PyRadiomics package (version 3.0.1, https://www.radiomics.io/), which is implemented in Python 3.8.0, and a p-value of less than 0.05 is considered statistically significant.

Results

Clinic features

The training and validation cohorts comprised 150 patients (70 males, 80 females; mean age, 50.3 ± 2.1 years; range, 31 to 69 years) and 52 patients (29 males, 22 females; mean age, 62.9 ± 1.7 years; range, 52 to 80 years), respectively. The difference was not statistically significant ($p = 0.217$).

The clinic features of the training and validation group are shown in Table 1. Among the analyzed variables, there was a statistically significant difference between the two groups of patients in terms of BMI, presence of diabetes and hyperlipidemia, carotid intima-media thickness, lumen stenosis, and plaque site PSV ($p < 0.05$).The distribution of gender among the two groups of patients, as well as the presence of hypertension and coronary heart disease, and the ratio of PSV at the plaque site to PSA in the distal segment, showed no statistically significant differences ($p > 0.05$).

Radiomics score

The LASSO regression-selected 43 radiomics features were used to establish a kernel function SVM classifier (Figs. 3 and 4); the model parameters were: gamma, 0.05; epsilon, 0.1. The AUC of the training group for this model was 89.42% (95% CI: 80.74-98.10%), and the AUC for the validation group was 82.73% (95% CI: 71.64-93.81%). The diagnostic performance of the SVM classifier in the training and validation groups is shown in Table 2, and the ROC curve is shown in Fig. 5.

Clinical usefulness

Both the radiomics nomogram and clinical nomogram showed good agreement in detecting the stability of plaque between prediction and histopathologic confirmation based on surgical specimens. The clinical usefulness of the two nomograms was evaluated using DCA (Fig. 6). The DCA curves showed that if the threshold probability was > 20%, using the radiomics nomogram to

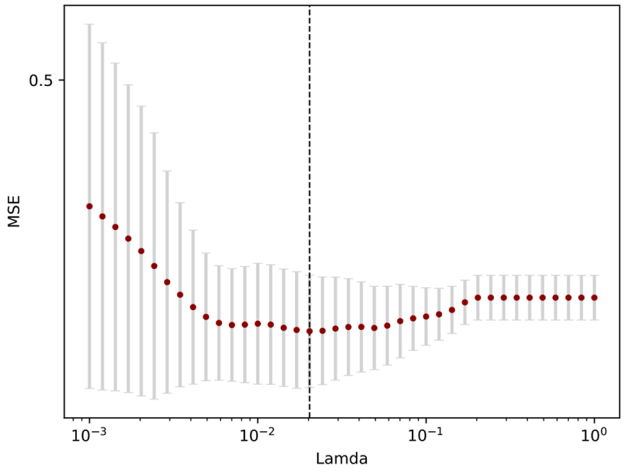

Fig. 3 Radiomics feature selection using the least absolute shrinkage and selection operator (LASSO) regression model in the training cohort. The 10-fold cross-validation (CV) process was repeated 40 times to generate the optimal penalization coefficient lambda (λ) in the LASSO model. The value of λ that gave the minimum average binomial deviance was used to select features. Dotted vertical lines were drawn at the optimal values using the minimum criteria and the 1 standard error of the minimum criteria (the 1-SE criteria). A λ value of 0.0203 was chosen (the 1-SE criteria) according to 10-fold CV, where optimal λ resulted in six nonzero coefficients

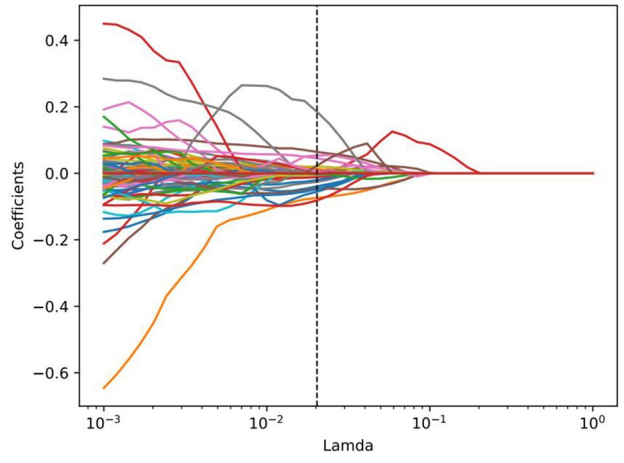

Fig. 4 The dynamic process diagram of radiomics feature selection using the least absolute shrinkage and selection operator (LASSO) regression model in the training cohort

predict stability of plaque added more benefit for patients than using the clinical nomogram.

Discussion

This study employed color Doppler ultrasound to examine the carotid arteries and combined AI techniques to automatically segment plaques and construct a corresponding model. The results demonstrated that the model achieved high levels of sensitivity (79.84% in the training group and 81.82% in the validation group) and specificity (93.10% in the training group and 80.00% in the validation group). Compared with the reference standard obtained manually by experienced physicians, the segmentation algorithm was effectively validated in terms of sensitivity and specificity, with results closely approximating the reference standard [36–38]. Moreover, through radiomics analysis of vulnerable plaques, this study extracted information of medical value, significantly enhancing the accuracy of plaque characterization. The application of this method not only reduced human errors but also shortened the time consumption in clinical workflow, showcasing the great potential of AI in medical image analysis. By applying AI-based plaque segmentation technology to the front-end processing of radiomics, this study provided an efficient and accurate method for medical image analysis. The updated guidelines for the early management of acute ischemic stroke emphasize the importance of early diagnosis and intervention [39]. Comprehensive reviews on carotid plaque vulnerability and its impact on ischemic stroke further highlight the clinical significance of our findings [40].

However, several limitations were also noted in this study. First, as a retrospective study, inherent biases may have affected the reliability of the results. Variations in ultrasound image quality, as well as differences among radiologists and ultrasound machines, could introduce heterogeneity, thereby influencing the performance of radiomics scores. This dependence on operators and equipment may be the primary reason for the less-than-ideal AUC values. Second, the study was conducted within a single institution, limiting the generalizability of the findings. Although the radiomics nomogram was validated in an internal cohort, further external validation across different centers is crucial to confirm its reliability. Additionally, the application of radiomics technology relies on specific technical expertise, including feature extraction software and statistical analysis skills [41]. To

Table 2 Diagnostic performance of the SVM classifier in the training and validation groups of artificial intelligence-segmented plaque ultrasound images

Groups	Sensitivity	Specificity	PPV	NPV	AUC(95% CI)
Training Group	79.84%	93.10%	75.56%	83.72%	89.42%(80.74-98.10%)
Testing Group	81.82%	80.00%	75.00%	78.13%	82.73%(71.64-93.81%)

Note: PPV—Positive Predictive Value; NPV—Negative Predictive Value; CI—Confidence Interval

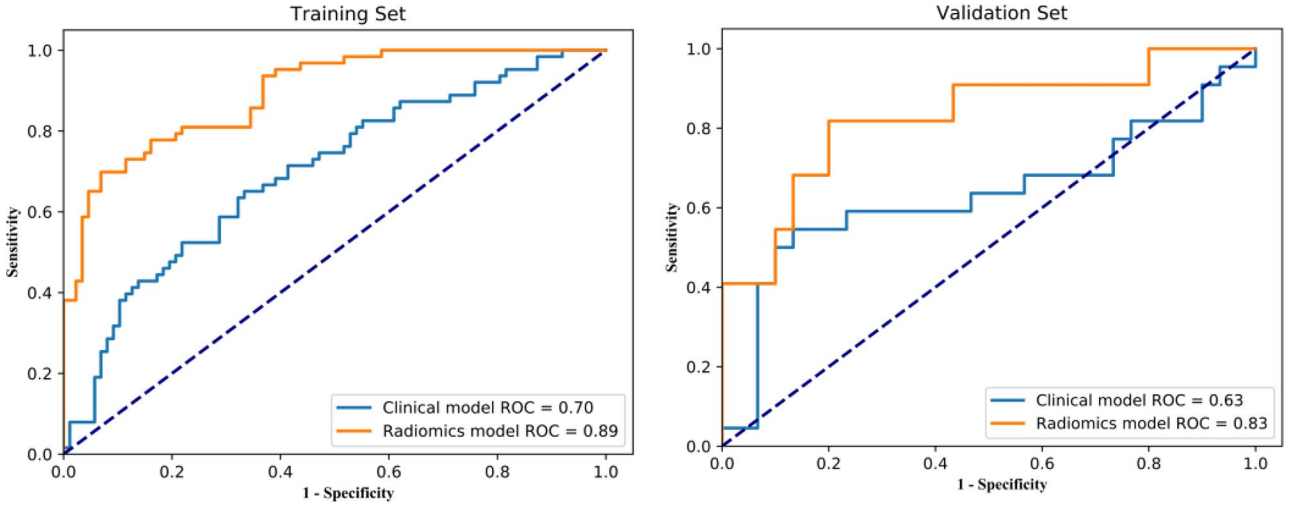

Fig. 5 ROC curves of the radiomics nomogram (orange curves) and clinical nomogram (blue curves) derived from the training and validation cohorts

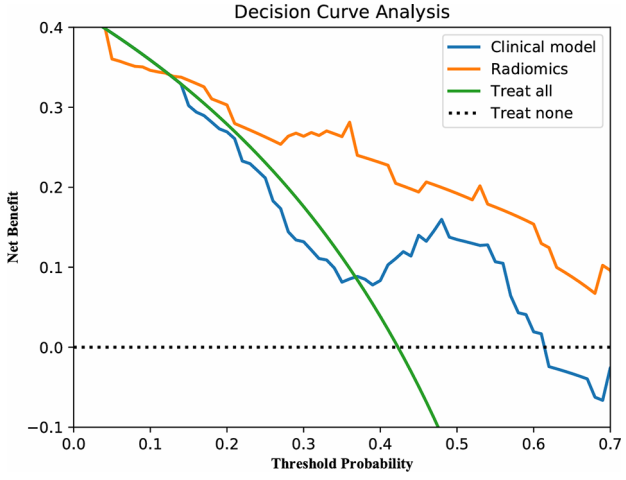

Fig. 6 Decision curve analysis (DCA) derived from the validation cohort. The y-axis measures the net benefit. The net benefit is determined by calculating the difference between the expected benefit and the expected harm associated with each proposed model [Net benefit = true positive rate – (false positive rate × weighting factor), weighting factor = threshold probability / (1-threshold probability)]. The green line represents the assumption that all patients were positive (the treat-all scheme). The black dashed line represents the assumption that all patients were negative (the treat-none scheme). If the threshold probability was > 20%, using the radiomics nomogram (orange curve) to predict vulnerable plaques added more benefit for patients than using the clinical nomogram (blue curve)

facilitate broader clinical adoption, radiomics technology needs to become more accessible and user-friendly.

Additionally, this study has certain limitations in terms of innovation. Although the application of AI in medical image analysis has made significant progress, the methods and techniques employed in this study are to some extent extensions of existing technologies. Future research needs to further explore new algorithms and technologies to achieve more precise and efficient medical image analysis. At the same time, attention must also be paid to the challenges faced in the application of AI in the medical field, such as data quality and privacy issues, to ensure the sustainable development and safe clinical application of the technology [42].

Despite these limitations, the results of this study are still impactful. By applying AI-based plaque segmentation technology to the front-end processing of radiomics, this study provided an efficient and accurate method for medical image analysis. Compared with traditional manual segmentation methods, AI technology not only improved work efficiency but also minimized the impact of human factors on diagnostic outcomes [43]. Moreover, this study demonstrated the potential of AI in the field of medical imaging, offering new ideas and directions for future research.

Future research directions should include the following aspects. First, well-designed prospective studies should be conducted to consider potential confounding factors such as operators, ultrasound machines, and other variables to improve the diagnostic accuracy of radiomics scores. Second, the scope of research should be expanded to include external validation across different centers to confirm the reliability of the radiomics nomogram. Additionally, future studies could explore the integration of imaging data with biomarkers, genomics, proteomics, and metabolomics data to enhance the predictive power of machine learning algorithms. This multimodal data fusion approach holds promise for providing more personalized healthcare solutions for patients [44].

Conclusion

In this research, we have constructed a radiomics scoring system based on ultrasound images of carotid plaques, which has the potential to be a biomarker for assessing plaque stability [45]. By combining the radiomics score with existing clinical risk factors, the nomogram

we developed using radiomics data demonstrates better performance in evaluating plaque stability than the conventional clinical nomogram. Therefore, this radiomics-based nomogram is expected to be a beneficial tool for predicting plaque stability, aiding in the early detection of ischemic stroke, risk assessment, and the formulation of treatment plans.

Acknowledgements
None.

Author contributions
Conception and design of the research: KLG and JLQ; acquisition of data: JJS, XYW, and LWZ; analysis and interpretation of data: JJS, LWZ, XYW and YL; statistical analysis: JJS, LWZ, YL, KLG and JLQ; drafting the manuscript: JJS, and LWZ; revision of manuscript for important intellectual content: KLG and JLQ. All authors read and approved the final manuscript.

Funding
This study was supported by National Natural Science Foundation of China (No. 82402970).

Data availability
The dataset used and/or analysed during the current study are available from the corresponding author on a reasonable request.

Declarations

Ethics approval and consent to participate
The research was performed in accordance with relevant guidelines and regulations, and granted ethical approval by the review board of Affiliated Nanjing Brain Hospital, Nanjing Medical University. For this retrospective study, obtaining informed consent was exempted.

Consent for publication
Not applicable.

Competing interests
The authors declare no competing interests.

Author details
[1]Department of Physical Diagnosis, Affiliated Nanjing Brain Hospital, Nanjing Medical University, No. 264, Guangzhou Road, Gulou District, Nanjing, Jiangsu 210008, China
[2]School of Mathematics, Nanjing University, Nanjing 210093, China
[3]School of Mathematics and Statistics, Nanjing University of Science and Technology, Nanjing 210094, China
[4]Department of Neurology, Affiliated Nanjing Brain Hospital, Nanjing Medical University, Nanjing 210008, China
[5]Department of Ultrasound Medicine, Affiliated Hospital of Medical School, Nanjing Drum Tower Hospital, Nanjing University, Nanjing 210000, China

Received: 22 November 2024 / Accepted: 26 February 2025
Published online: 17 March 2025

References

1. Biscetti F, Tinelli G, Rando MM, Nardella E, Cecchini AL, Angelini F, et al. Association between carotid plaque vulnerability and high mobility group box-1 serum levels in a diabetic population. Cardiovasc Diabetol. 2021;20(1):114. https://doi.org/10.1186/s12933-021-01304-8.
2. Shin JJ, Hachinski V, Azarpazhooh MR, Shariatzadeh A, Spence JD. Measurement of carotid plaque burden: A tool for predicting and preventing dementia? Cereb circulation - cognition Behav. 2021;2:100004. https://doi.org/10.1016/j.cccb.2021.100004.
3. Azzopardi C, Camilleri KP, Hicks YA. Bimodal automated carotid ultrasound segmentation using geometrically constrained deep neural networks. IEEE J Biomedical Health Inf. 2020;24(4):1004–15. https://doi.org/10.1109/jbhi.2020.2965088.
4. Choi Y, Won KB, Kang HH, Change HJ. Association of serum hemoglobin level with the risk of carotid plaque beyond metabolic abnormalities among asymptomatic adults without major adverse clinical events: a cross-sectional cohort study. BMC Cardiovasc Disord. 2021;21(1):35. https://doi.org/10.1186/s12872-021-01852-7.
5. Simonetto M, Dharmadhikari S, Bennett A, Campo N, Asdaghi N, Romano J, et al. Do carotid plaque ulcers heal?? Potential detection of carotid artery plaque heal?ing by carotid ultrasound imaging. J Ultrasound Medicine: Official J Am Inst Ultrasound Med. 2021;40(5):973–80. https://doi.org/10.1002/jum.15472.
6. Powers WJ, Rabinstein AA, Ackerson T, Adeoye OM, Bambakidis NC, Becker K, et al. Guidelines for the early management of patients with acute ischemic stroke: 2019 update to the 2018 guidelines for the early management of acute ischemic stroke: A guideline for healthcare professionals from the American heart association/american stroke association. Stroke. 2019;50(12):e344–418. https://doi.org/10.1161/str.0000000000000211.
7. Brunner C, Denis NL, Gertz K, Grillet M, Montaldo G, Endres M, et al. Brain-wide continuous functional ultrasound imaging for real-time monitoring of hemodynamics during ischemic stroke. J Cereb Blood Flow Metab. 2024;44(1):6–18. https://doi.org/10.1177/0271678x231191600.
8. Baradaran H, Foster T, Harrie P, McNally JS, Alexander M, Pandya A, et al. Carotid artery plaque characteristics: current reporting practices on CT angiography. Neuroradiology. 2021;63(7):1013–8. https://doi.org/10.1007/s00234-020-02610-w.
9. Kassem M, Florea A, Mottaghy FM, van Oostenbrugge R, Kooi ME. Magnetic resonance imaging of carotid plaques: current status and clinical perspectives. Ann Transl Med. 2020;8(19):1266. https://doi.org/10.21037/atm-2020-cass-16.
10. Lepor NE, Sun J, Canton G, Contreras L, Hippe DS, Isquith DA, et al. Regression in carotid plaque lipid content and neovasculature with PCSK9 Inhibition: A time course study. Atherosclerosis. 2021;327:31–8. https://doi.org/10.1016/j.atherosclerosis.2021.05.008.
11. Baradaran H, Gupta A. Extracranial vascular disease: carotid stenosis and plaque imaging. Neuroimaging Clin N Am. 2021;31(2):157–66. https://doi.org/10.1016/j.nic.2021.02.002.
12. Li Q, Liu B, Zhao Y, Liu Y, Gao M, Jia L, et al. Echolucent carotid plaque is associated with restenosis after carotid endarterectomy. J Neurosurg. 2021;134(3):1203–9. https://doi.org/10.3171/2020.2.Jns193397.
13. Saba L, Cau R, Murgia A, Nicolaides AN, Wintermark M, Castillo M, et al. Carotid Plaque-RADS: A novel stroke risk classification system. JACC Cardiovasc Imaging. 2024;17(1):62–75. https://doi.org/10.1016/j.jcmg.2023.09.005.
14. Zhou M, Wang H, Zeng X, Yin P, Zhu J, Chen W, et al. Mortality, morbidity, and risk factors in China and its provinces, 1990–2017: a systematic analysis for the global burden of disease study 2017. Lancet. 2019;394(10204):1145–58. https://doi.org/10.1016/s0140-6736(19)30427-1.
15. Bohlender S, Oksuz I, Mukhopadhyay A. A survey on Shape-Constraint deep learning for medical image segmentation. IEEE Rev Biomed Eng. 2023;16:225–40. https://doi.org/10.1109/rbme.2021.3136343.
16. Zhao D, Wang W, Tang T, Zhang YY, Yu C. Current progress in artificial intelligence-assisted medical image analysis for chronic kidney disease: A literature review. Comput Struct Biotechnol J. 2023;21:3315–26. https://doi.org/10.1016/j.csbj.2023.05.029.
17. Jain NK, Singh G, Muralidharan CG, Gupta A, Chatterjee S, Rajesh U. Assessment of plaque vulnerability in carotid atherosclerotic plaques using contrast-enhanced ultrasound. Medical journal. Armed Forces India. 2022;78(4):422–9. https://doi.org/10.1016/j.mjafi.2020.09.013.
18. Zhou F, Hua Y, Ji X, Jia L. A systemic review into carotid plaque features as predictors of restenosis after carotid endarterectomy. J Vasc Surg. 2021;73(6):2179–88. https://doi.org/10.1016/j.jvs.2020.10.084.
19. Chen X, Wang X, Zhang K, Fung KM, Thai TC, Moore K, et al. Recent advances and clinical applications of deep learning in medical image analysis. Med Image Anal. 2022;79:102444. https://doi.org/10.1016/j.media.2022.102444.
20. Fabiani I, Palombo C, Caramella D, Nilsson J, De Caterina R. Imaging of the vulnerable carotid plaque: role of imaging techniques and a research agenda. Neurology. 2020;94(21):922–32. https://doi.org/10.1212/wnl.0000000000009480.
21. Nobre Menezes M, Silva B, Silva JL, Rodrigues T, Marques JS, Guerreiro C, et al. Segmentation of X-ray coronary angiography with an artificial intelligence

deep learning model: impact in operator visual assessment of coronary stenosis severity. Catheterization Cardiovasc Interventions: Official J Soc Cardiac Angiography Interventions. 2023;102(4):631–40. https://doi.org/10.1002/ccd.30805.
22. Scicolone R, Vacca S, Pisu F, Benson JC, Nardi V, Lanzino G, et al. Radiomics and artificial intelligence: general notions and applications in the carotid vulnerable plaque. Eur J Radiol. 2024;176:111497. https://doi.org/10.1016/j.ejrad.2024.111497.
23. Vacca S, Scicolone R, Gupta A, Allan Wasserman B, Song J, Nardi V, et al. Atherosclerotic carotid artery disease radiomics: A systematic review with meta-analysis and radiomic quality score assessment. Eur J Radiol. 2024;177:111547. https://doi.org/10.1016/j.ejrad.2024.111547.
24. Dundas J, Leipsic JA, Sellers S, Blanke P, Miranda P, Ng N, et al. Artificial Intelligence-based coronary stenosis quantification at coronary CT angiography versus quantitative coronary angiography. Radiol Cardiothorac Imaging. 2023;5(6):e230124. https://doi.org/10.1148/ryct.230124.
25. Collaborators GN. Global, regional, and National burden of neurological disorders, 1990–2016: a systematic analysis for the global burden of disease study 2016. Lancet Neurol. 2019;18(5):459–80. https://doi.org/10.1016/s1474-4422(18)30499-x.
26. Lauricella A, Berchiolli R, Moratto R, Ferri M, Viazzo A, Silingardi R. Impact of plaque dilation before carotid artery stent deployment. J Vasc Surg. 2020;71(3):842–53. https://doi.org/10.1016/j.jvs.2019.05.048.
27. Tschiderer L, Klingenschmid G, Seekircher L, Willeit P. Carotid intima-media thickness predicts carotid plaque development: Meta-analysis of seven studies involving 9341 participants. Eur J Clin Invest. 2020;50(4):e13217. https://doi.org/10.1111/eci.13217.
28. Kasashima K, Fujimoto M, Tani S, Ogata H, Shimizu K, Itani M, et al. Symptomatic atherosclerotic plaque accompanied by carotid web. Neuroradiol J. 2023;36(2):220–3. https://doi.org/10.1177/19714009221122192.
29. Naqvi TZ. Multimodality imaging classification for carotid plaque assessment. JACC Cardiovasc Imaging. 2024;17(1):76–8. https://doi.org/10.1016/j.jcmg.2023.11.004.
30. Zhang L, Li X, Lyu Q, Shi G. Imaging diagnosis and research progress of carotid plaque vulnerability. J Clin Ultrasound: JCU. 2022;50(7):905–12. https://doi.org/10.1002/jcu.23266.
31. Mekke JM, Egberts DHJ, Waissi F, Timmerman N, Bot I, Kuiper J, et al. Mast cell distribution in human carotid atherosclerotic plaque differs significantly by histological segment. Eur J Vascular Endovascular Surgery: Official J Eur Soc Vascular Surg. 2021;62(5):808–15. https://doi.org/10.1016/j.ejvs.2021.07.008.
32. Benson JC, Cheek H, Aubry MC, Lanzino G, Huston Iii J, Rabinstein A, et al. Cervical carotid plaque MRI: review of atherosclerosis imaging features and their histologic underpinnings. Clin Neuroradiol. 2021;31(2):295–306. https://doi.org/10.1007/s00062-020-00987-y.
33. Fukushima D, Kondo K, Harada N, Terazono S, Uchino K, Shibuya K, et al. Quantitative comparison between carotid plaque hardness and histopathological findings: an observational study. Diagn Pathol. 2022;17(1):58. https://doi.org/10.1186/s13000-022-01239-y.
34. Giannopoulos AA, Kyriacou E, Griffin M, Pattichis CS, Michael J, Richards T, et al. Dynamic carotid plaque imaging using ultrasonography. J Vasc Surg. 2021;73(5):1630–8. https://doi.org/10.1016/j.jvs.2020.10.021.
35. Zhou R, Azarpazhooh MR, Spence JD, Hashemi S, Ma W, Cheng X, et al. Deep Learning-Based carotid plaque segmentation from B-Mode ultrasound images. Ultrasound Med Biol. 2021;47(9):2723–33. https://doi.org/10.1016/j.ultrasmedbio.2021.05.023.
36. Benson JC, Nardi V, Hunt CH, Lerman A, Lanzino G, Brinjikji W. Cardiovascular risk factors and cervical carotid plaque features on CT angiography. Neuroradiol J. 2022;35(3):346–51. https://doi.org/10.1177/19714009211047450.
37. Li Y, Zheng S, Zhang J, Wang F, He W. Multimodal ultrasound parameters aided carotid plaque risk stratification in patients with asymptomatic carotid stenosis. Acta Radiol (Stockholm Sweden: 1987). 2022;63(2):278–86. https://doi.org/10.1177/0284185121989189.
38. Phyo WSY, Shirakawa M, Yamada K, Kuwahara S, Yoshimura S. Characteristics of calcification and their association with carotid plaque vulnerability. World Neurosurg. 2022;167:e1017–24. https://doi.org/10.1016/j.wneu.2022.08.127.
39. Park HK, Ko SB, Jung KH, Jang MU, Kim DH, Kim JT, et al. 2022 Update of the Korean clinical practice guidelines for stroke: antithrombotic therapy for patients with acute ischemic stroke or transient ischemic attack. J Stroke. 2022;24(1):166–75. https://doi.org/10.5853/jos.2021.02628.
40. Pias AD, Pereira-Macedo J, Marreiros A, António N, Rocha-Neves J. Advancing vascular surgery: the role of artificial intelligence and machine learning in managing carotid stenosis. Portuguese J Cardiac Thorac Vascular Surg. 2024;31(3):55–64. https://doi.org/10.48729/pjctvs.411.
41. Shan D, Wang S, Wang J, Lu J, Ren J, Chen J, et al. Computed tomography angiography-based radiomics model for predicting carotid atherosclerotic plaque vulnerability. Front Neurol. 2023;14:1151326. https://doi.org/10.3389/fneur.2023.1151326.
42. Meshram NH, Mitchell CC, Wilbrand S, Dempsey RJ, Varghese T. Deep learning for carotid plaque segmentation using a dilated U-Net architecture. Ultrason Imaging. 2020;42(4–5):221–30. https://doi.org/10.1177/0161734620951216.
43. Li J, Li D, Yang D, Hang H, Wu Y, Yao R, et al. Irregularity of carotid plaque surface predicts subsequent vascular event: A MRI study. J Magn Reson Imaging: JMRI. 2020;52(1):185–94. https://doi.org/10.1002/jmri.27038.
44. Baradaran H, Sarrami AH, Gupta A. Asymptomatic carotid disease and cognitive impairment: what is the evidence?? Frontiers in neurology. 2021;12:741500. https://doi.org/10.3389/fneur.2021.741500
45. Chen J, Wang B, Song J, Qi Z, Deng Y. Multiple techniques to evaluate the relationship between carotid artery plaque and acute stroke. Clin Hemorheol Microcirc. 2024;86(3):327–37. https://doi.org/10.3233/ch-231959.

Publisher's note